Heliyon 10 (2024) e32795

Contents lists available at ScienceDirect

Heliyon

journal homepage: www.cell.com/heliyon

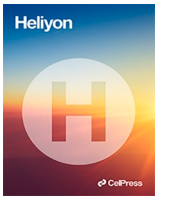

Research article

High-performance CO detection based on a PhC cavity in terahertz band

Qi Cheng [a,*], Yuanlin Guan [a], Guangsheng Xu [a], Jianlin Dong [a], Na Liu [b]

[a] Mechanical and Automotive Engineering, Qingdao University of Technology, Qingdao 266520, Shandong, China
[b] Measurement Technology and Instrumentation Key Lab of Hebei Province, Yanshan University, Qinhuangdao 066004, China

ARTICLE INFO

Keywords:
Photonic crystal cavity
Carbon monoxide sensing
Slot structure
Terahertz band

ABSTRACT

Combined with the light absorption from molecular vibration, photonic crystal (PhC) cavity structures have gradually shown great potential in gas detection, particularly for toxic gases. We proposed a PhC cavity with a high-quality factor of 1.24×10^6 and a small mode volume of 2.3×10^{-4} $(\lambda/n)^3$, which was used for carbon monoxide detection. To reduce the interference of other gases, we set the resonance frequency in the terahertz band. The numerical analysis shows that the structure has good selectivity and high sensitivity, and the linear fitting of the results provides the possibility to realize the application, which has great competitiveness in the same type of sensor structure. Additionally, we also proved that the interference of H_2O and CO_2 on the CO sensing can be ignored, and it supports the detection of CO without pre-drying.

1. Introduction

In recent years, there have been frequent occurrences of CO poisoning in automobiles, thus the effective detection of CO is an important measure to ensure the safety of life. Most of the traditional gas detection methods are based on the electrochemical characteristics of gases [1,2]. Although electrochemical gas sensors can achieve high sensitivity (*S*) and high resolution, most of them have the characteristics of short service life and susceptibility to environmental influences. Furthermore, this method is usually based on large-scale laboratory analysis equipment such as gas chromatographs, and it is usually impossible to obtain real-time data. In addition, another substance may be required as a label to mark the analyte, which increases the interference and complexity of the operation [3,4].

Recently, optical sensors based on photonic crystal (PhC) cavities have shown broad application prospects because of their high sensitivity, high selectivity, and excellent manipulation of light on the nanoscale [5–9]. For these structures, high-quality factor (*Q*) and small mode volume (*V*) mean strong light-matter interaction, which is a necessary condition for effectively limiting light energy and achieving highly sensitive gas detection with a low limit of detection (LoD). However, the current sensing mechanism of most PhC cavity sensors is mainly based on the sensing of changes in refractive index to achieve the detection of the analyte, which is called a refractive index sensor. By realizing high *Q*/*V* values, the sensitivity to refractive index changes can be improved by optimizing the dielectric PhC structures. Yang et al. presented high-*Q* PhC dielectric cavities for refractive index sensing, and the *Q* factor of 2.1×10^5 and S of 563.6 nm/RIU can be estimated [10]. Feng et al. have proposed a new ultracompact optical gas sensor based on PhC nanobeam cavity coupled to tapered fiber, with a *Q* factor of 2.2×10^6 and *V* of $0.29(\lambda/n)^3$ by Finite-difference time-domain (FDTD) method, and

* Corresponding author.
E-mail address: chengqi@qut.edu.cn (Q. Cheng).

https://doi.org/10.1016/j.heliyon.2024.e32795
Received 29 January 2024; Received in revised form 20 May 2024; Accepted 10 June 2024
Available online 11 June 2024

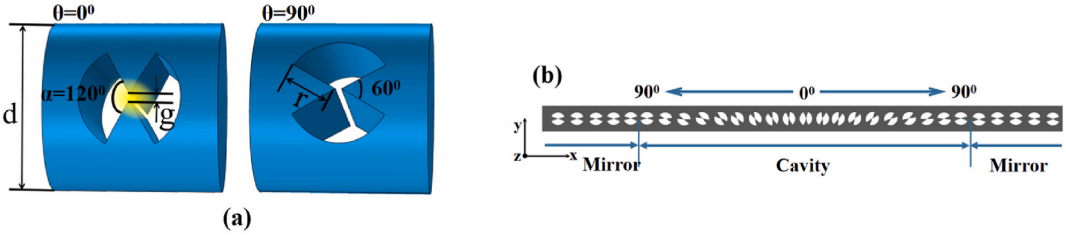

Fig. 1. 1D PhC cavity design based on a bow-tie unit cell. (a) The bow-tie unit cell with rotation angle θ of 0° and 90°. (b) The proposed PhC cavity is composed of a silicon bowtie unit cell with gradually rotating angles (10-degree rotation per unit cell).

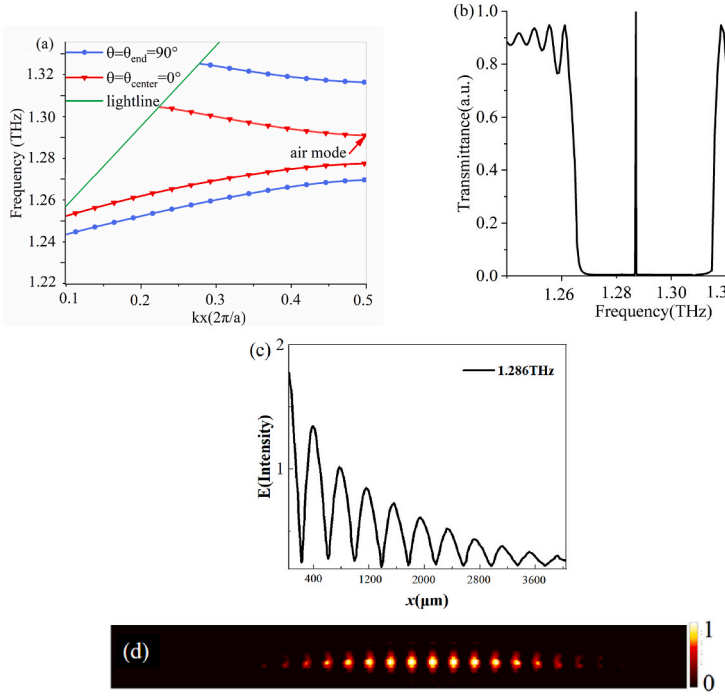

Fig. 2. Results of the designed structure without any gas filled. (a) The band structure diagram in TE light. The red lines represent the two modes of bow-tie unit cell with $\theta = \theta_{center} = 0°$ and the blue lines represent the two modes of bow-tie unit cell with $\theta = \theta_{end} = 90°$. (b) At 1.286 THz, a sharp peak occurs in the transmittance spectrum of the cavity without any gas filled. (c) The magnitude of the electric field along the *x* axis. (d) The electric field map in a resonance frequency of 1.286 THz.

the S of 190nm/RIU is obtained [11]. However, this type of sensor has great limitations for the identification of mixed gases and the further improvement of sensing property due to the diffraction limit [12]. Although surface plasmon-based hybrid cavity structures have been proposed, which can break the diffraction limit to achieve a smaller V value, most of them have large ohmic losses due to the existence of metal structures, which will seriously affect signal transmission.

In addition, although many sensors in the infrared and ultraviolet bands have been widely studied and applied, this type of gas sensor still underperforms in terms of sensitivity and mixed gas recognition [13]. Therefore, utilizing the absorption characteristics of CO gas, we set the resonant frequency of the microcavity in the terahertz band instead of the ultraviolet/visible light and infrared electromagnetic regions, which can reduce the influence of interfering gases and improve the selectivity of the sensor. Although Shi et al. have obtained a sensing structure for gas detection in the terahertz band using a 1D PhC cavity composed of a stack of silicon wafers, it is not desirable in practical application because it cannot obtain good linear correspondence [14]. Compared with their structure, we proposed a dielectric PhC cavity based on a suspended optical fiber, which not only solved the physical limitations of the ordinary dielectric cavities and plasmonic cavities but also is more conducive to coupling with other devices with lower coupling loss. Our structure is composed of a cyclically varying bow-tie structure with the interlocking effect from the slot and the anti-slot structure. It has a strong optical localization effect, and an ultra-high *Q/V* value is therefore achieved. Comprehensively, combined with a high-performance cavity structure, it is feasible to achieve high selectivity, high S, and low LoD detection of CO gas.

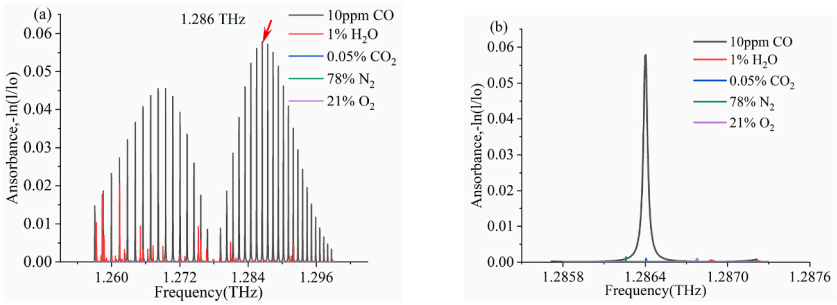

Fig. 3. The absorbance spectra of different gases at the pressure of 1 atm and the temperature of 296 K. (a) The absorbance spectra of five gases (10 ppm CO, 1 % H_2O, 0.05 % CO_2, 78 % N_2, 21 % O_2). (b) The magnified view of absorbance spectra at 1.286 THz for easier observation.

2. Theoretical design of the cavity and applications in CO sensing

To achieve highly sensitive and highly selective sensing based on a suspended optical fiber, a cavity with an ultra-high *Q* and small *V* plays a key role. Compared with traditional resonant cavities, the slot structure has been documented to have strong optical confinement capability [15,16]. At the same time, Shuren et al. have proposed the anti-slot concept, which has a certain significance in cavity design [17]. According to this view, when an infinite number of interlocking anti-slots and slots are introduced to the unit cell to form a bow-tie shape, the light can be squeezed in a direction parallel or perpendicular to its propagation direction. Compared with plasma bow ties, the all-dielectric bow tie structure can support design freedom and fabrication tolerance, enabling extreme optical confinement in the air gap on both sides of the bow tie while maintaining high *Q*. However, *Q* is ultimately limited in practice by other factors, such as bandwidth considerations, material absorption, or fabrication tolerances, minimizing Vmode for a given Q is a preferred solution with practical applications in mind.

The unit cell with a bow-tie shape is illustrated in Fig. 1(a), and the interlocking geometry ends with an air gap, in which the light can be confined strongly to support stronger light-matter interactions. There is a 15 μm wide gap (*g*) between the tips of two sectors with a radius (*r*) of 152 μm and an angle (α) of 120°. As shown in Fig. 1(b), based on the optical fiber with a diameter (*d*) of 380 μm, the designed PhC cavity is composed of bow-tie cells with a period of 400 μm (The selection of structural parameters is shown in the supplementary file). The rotating angle α of each cell is from 0° to 90° with an interval of 10°. The two mirrors on both sides of the PhC cavity contain five bow-tie cells with the same rotating angle of 90°. In this paper, the cyclic olefin polymer (COC, TOPAS material) with better optical properties is chosen to replace the conventional glass material, which has an average absorption coefficient of 0.2 cm^{-1} in the range of 0.2 THz~ 5.0 THz and its refractive index remains essentially constant around 1.53 in the frequency domain of 0.1 THz~ 2 THz. The terahertz light source can choose the Germany BATOP FC-TDS all fiber type THz-TDS system, and its band range is 0.05 THz-1.5 THz, which can meet the requirements of subsequent experiments. Based on the theoretical design, we preliminarily used reactive ion etching combined with dry etching to realize the preparation of suspended fiber microcavity [18,19]. Of course, this is only our preliminary idea, and the details will depend on the specific situation.

Fig. 2(a) shows the calculated photonic band gaps (PBGs) in the TE band diagram based on 3D-FDTD numerical method, which contains the first two bands closest to the PBG of dielectric bow-tie unit cells. The PBG with $\theta_{center} = 0°$ (red line) is narrower than the one with $\theta_{end} = 90°$ (blue line), and the air band of the unit cell with $\theta_{center} = 0°$ lies in the middle of the PBG with $\theta_{end} = 90°$. Therefore, it is possible to use two symmetrical mirrors to limit the edge mode of the central cavity [20]. The TE polarized light source with a wavelength range of 0.2 THz-5THz is used and the transmission spectra can be obtained by the monitor of the output port. The transmittance spectrun of the designed cavity without any gas filling is shown in Fig. 2(b). There is a sharp peak at 1.286 THz in a broad band from 1.269 THz to 1.316 THz. The broadband not only provides a wide monitoring wavelength range but also greatly expands the application range of the cavity. The distribution of the electric field magnitude of the reflector at a wavelength of 1.286 THz along the *x* axis, which is just at the center of the bandgap, is displayed in the lower panel of Fig. 2(c). It can be observed that the electric field strength decays drastically into the mirror, revealing its capability of realizing an ultrasmall microcavity. It also shows that the penetrating length of the reflector, through which the magnitude of the electric field decreases to 1/e of the original, is around four periods. In order to further improve the optical localization capability, we increased the number of periods to 5. The corresponding electric field map at the resonance frequency of 1.286 THz is also described in Fig. 2(d). The *Q* value of 1.24×10^6 and the *V* of $2.3 \times 10^{-4}(\lambda/n)^3$ can be calculated by the following equation [21]:

$$Q = \frac{-2\pi f_R \log_{10}(e)}{2m} \tag{1}$$

where f_R is the resonance frequency of the mode, and *m* is the slope of the log of the time signal envelope. The mode volume *V* is calculated by Ref. [22]:

$$V = \frac{\int \varepsilon |E|^2 dV}{\max\left(\varepsilon |E|^2\right)} \tag{2}$$

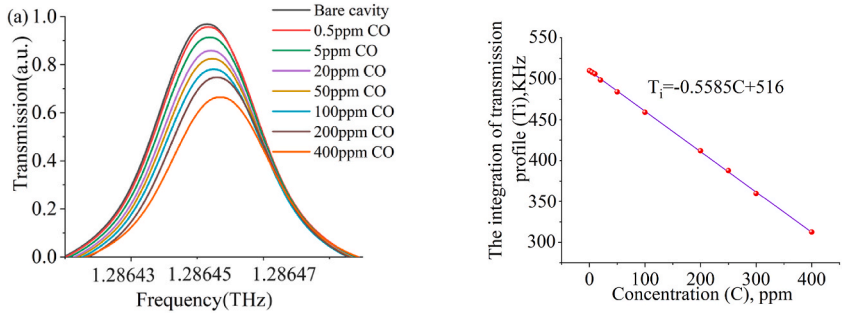

Fig. 4. The results of the cavity for different CO concentrations. (a) Transmission spectra of the PhC cavity filled with different concentrations of CO diluted in air at 1 atm and 296 K. (b) The integration of transmission profile (Ti) is linearly decayed as a function of CO concentration (C) represented in red balls, and the fitting curve is also shown in the picture represented in blue lines.

The more concentrated the light field of the resonant cavity, the smaller the effective V of the cavity.

It is known that the terahertz band has relatively less interference from other gases for CO detection compared to the near- and mid-infrared bands. Fig. 3(a) demonstrates the absorbance spectra of 10 ppm CO and four main gases in air (1 % H_2O, 0.05 % CO_2, 78 % N_2, 21 % O_2) at the pressure of 1 atm and the temperature of 296 K in the terahertz band based on the HITRAN database (http://www.hitran.org/). For easy observation, an enlarged view of the absorbance peak near 1.286 THz is shown in Fig. 3(b). There is an obvious absorption peak of the target gas CO with little influence from other gases. Therefore, the proposed cavity with a resonant frequency of 1.286 THz is feasible for CO detection.

When the cavity is filled with CO, the intrinsic loss caused by the rotational resonance of CO at the resonance frequency will significantly affect the transmission spectra. To simulate the change of the transmission spectra more accurately, the Lorentz oscillator model of classical dispersion theory can be used to describe the permittivity of gases [23]:

$$\varepsilon_r(\omega) = \varepsilon_\infty + \sum_{p=1}^{P} \frac{\Delta\varepsilon_p \omega_p^2}{\omega_p^2 - \omega^2 - i\gamma_p \omega} \tag{3}$$

where ε_∞ is set to 1 as the background permittivity of the gas, which sets a baseline for the real part of the dielectric constant across frequency, ω_p is the angular frequency, $\Delta\varepsilon_p$ is the change in the relative permittivity and it is equivalent to the strength of the mode, which is a function of the gas concentration (C) and the gas pressure (P), γ_p is the damping coefficient ($P \times 2 \times$ pi $\times$ 6 MHz/hPa) which is only dependent on the overall pressure. Then, the Fourier transform is applied to the transmission spectra, and the Lorentz parameters can be calculated by fitting the curve using the parametric techniques for the transmission spectra. Finally, the gas concentration can be obtained according to the molecular density. At the frequency of 1.286 THz, we can fit these parameters for diluted CO with a concentration of 10 ppm under the pressure of 1 atm, and find that $\Delta\varepsilon_p$ is equal to 2.8×10^{-9} [24].

3. Results and discussion

Based on the report from the World Health Organization, staying in a CO environment with a concentration of 50 ppm for half an hour is the maximum that humans can bear [25]. Usually, if the concentration of CO exceeds 100 ppm, it is extremely likely to be life-threatening. Therefore, it is imperative to be able to sense CO timely and sensitive. Fig. 4(a) depicts the transmission spectra of CO gas with different concentrations at the pressure of 1 atm and the temperature of 296 K. It shows that the peak of the transmission spectra is decreased with the increase of CO concentration, and the position of the peaks appears an obvious shift. This is mainly because the cavity mode with ultra-high Q/V value is very sensitive to the change of refractive index caused by gas concentration. Compared with the bare cavity (without any gas filling), the transmittance decreases from 0.99 to 0.98 when the CO concentration increases to 0.5 ppm. Fig. 4(b) shows the change of the integration in transmission profile (T_i) as the CO concentration (C) from 0.5 ppm to 400 ppm, where T_i is defined as the integral value of the spectrum in 1.2858 THz - 1.2870 THz. It can be observed that the curve decays linearly and the concentration of CO can be quantitatively analyzed by the fitted straight line, which can be described by $T_i = -0.5585C + 516$. The corresponding R-square (COD) of the fitting line is 0.999, which is close to 1, proving that the senor can support accurate quantitative analysis of CO. The sensitivity S can be simply defined as the slope of the fitted straight line. Therefore, the structure is more capable of achieving high S (558.5 a. u.Hz/ppm) in a CO environment with low concentration (0–400 ppm). In this work, we assume that the detectable transmittance change is 0.01, and the LoD can be as low as 0.5 ppm at a pressure of 1 atm and a temperature of 296 K.

Because the concentration of water vapor, that is, humidity, is greatly disadvantageous in the detection of gases. Here, to explore the influence of interfering gas on the detection of CO, the concentrations of H_2O and CO_2 are considered as variables in the following discussion. Applying the integrated spectroscopic model [26,27] based on the HITRAN database, the permittivity of the mixed gas specimen is a combination of contributions from CO, H_2O, and CO_2, which can be modeled using [14]:

$$\varepsilon_r = \varepsilon_\infty + P_{CO} + P_{H_2O} + P_{CO_2} \tag{4}$$

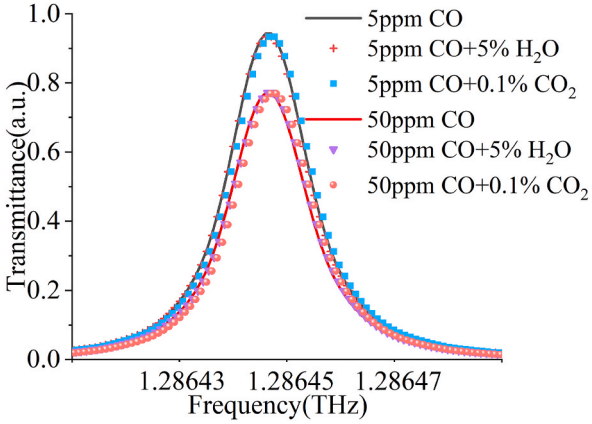

Fig. 5. Transmission spectra for six cases: the PhC cavity with only 5 ppm CO (black line); the PhC cavity with 5 ppm CO and 5 % H_2O (red plus sign); the PhC cavity with 5 ppm CO and 0.1 % CO_2 (blue tetragonum); the PhC cavity with only 50 ppm CO(red line); the PhC cavity with 50 ppm CO and 5 % H_2O (purple triangle); the PhC cavity with 50 ppm CO and 0.1 % CO_2 (red ball); All the calculations are at the conditions of 1 atm and 296 K.

Table 1
The comparison for characters of different gas sensor.

Reference	Sensitivity	LoD	Resistance to interference	Target gas
Ref. [26]	618.1/RIU	–	No	Not mentioned
Ref. [27]	2.3×10^5nmRIU^{-1}	2.08×10^{-7}RIU	No	H_2S
Ref. [28]	1.5028×10^5	6.67×10^{-11}RIU	Yes	CO
Ref. [29]	3200nm/RIU	–	No	Not mentioned
Ref. [30]	–	800 molecules	No	CO
Ref. [31]	64.28 %	–	No	CO
This work	558.5	0.5 ppm	Yes	CO

where P_{CO}, P_{H_2O}, and P_{CO_2} are the electric polarization from H_2O, CO, and CO_2, and the three quantities are both in the form of Lorentzian oscillators, ε_∞ is also set to 1.

In Fig. 3(a), we can see that the absorption intensity of 1 % H_2O and 0.05 % CO_2 is pretty weak, so it can be inferred that H_2O and CO_2 may have little effect on the detection of CO. Furthermore, after the above analysis and calculations, the obtained results are illustrated in Fig. 5. It is clear that under the same environmental conditions (the pressure is 1 atm and the temperature is 296 K), there is little change in the transmission spectra except that the peak position is slightly shifted to the right when 5 % H_2O and 0.1 % CO_2 are introduced into 5 ppm CO. To make sure that CO concentration sensing will not be affected by the presence of interfering gases, the CO concentration is changed from 5 ppm to 50 ppm when the H_2O concentration is 5 % and CO_2 concentration is 0.1 %. The obtained two transmission spectra are respectively represented by purple triangles and red balls, and both of them have a great decrease compared to the one with only 5 ppm CO (black line). In addition, the two spectral curves are similar to the one containing only 50 ppm CO (red line), but the peak position is slightly shifted to the right due to the change of the refractive index in the cavity. This indicates that the peaks of the transmission spectra greatly depend on the CO concentration, and H_2O and CO_2 have little interference with it.

Based on the above discussion, it can be learned that the proposed cavity can be directly used for CO detection without pre-drying, which reduces the possibility of introducing interfering substances. In addition, the cavity also has good immunity to CO_2 gas, ensuring the accuracy of CO detection. From another perspective, the results show that the designed cavity structure exhibits a strong selectivity ability in CO detection, which largely depends on its high Q value and small V, and therefore the designed PhC cavity may be used in CO identification. Furthermore, based on the cavity design method proposed in this work, the cavity can be used for the detection of other gases by adjusting its structural parameters, which needs further discussion (See Fig. S1 of the Supplementary file).

At present, most gas detection based on micro-nano optical structure is mainly based on its detection of gas refraction change. However, for trace gases, the refractive index change is too small to cause a large refractive index change, which seriously affects the detection sensitivity and limit of detection (LoD). Here, the gas detection reports in recent years are compared in Table 1. Although the result unit is not uniform, on the whole, our work has a unique advantage in gas detection because of its strong anti-interference.

4. Conclusions

In summary, we proposed a 1D PhC cavity operating in the terahertz band, which was used for CO gas sensing with high *S* and low *LoD*. The cavity was designed based on the slot and anti-slot concept, which consists of a series of bow-tie unit cells. There is an air gap in the center of the bow-tie unit cell, which can effectively confine the light energy and obtain strong light-matter interaction in air

mode. By symmetrically rotating the bow-tie unit cells, a bare cavity with a high Q value of 1.24×10^6 and a small V of 2.3×10^{-4} $(\lambda/n)^3$ is obtained. We found that the integration of transmittance spectra changes linearly with the sensitivity of 558.5a.u.Hz/ppm, and the *LoD* of 0.5 ppm can be obtained. We have also proved that there is little influence from water vapor and carbon dioxide. Therefore, the PhC cavity provides great convenience for CO detection without pre-drying and purification, which can avoid the introduction of unnecessary interfering substances.

Funding

This research was funded by the Natural Science Foundation of Qingdao (No.23-2-1-125-zyyd-jch and No.3-2-1-125-zyyd-jch).

CRediT authorship contribution statement

Qi Cheng: Writing – original draft, Supervision, Methodology. **Yuanlin Guan:** Conceptualization. **Guangsheng Xu:** Software. **Jianlin Dong:** Data curation. **Na Liu:** Writing – review & editing.

Declaration of competing interest

No conflict of interest exits in the submission of this manuscript, and manuscript is approved by all authors for publication. I would like to declare on behalf of my co-authors that the work described was original research that has not been published previously, and not under consideration for publication elsewhere, in whole or in part. All the authors listed have approved the manuscript that is enclosed.

Appendix A. Supplementary data

Supplementary data to this article can be found online at https://doi.org/10.1016/j.heliyon.2024.e32795.

References

[1] S.P. Wu, X. Zhong, Z. Qu, et al., Infrared gas detection and concentration inversion based on dual-temperature background points, Photnics 10 (5) (2023) 490.
[2] J.H. Yang, R.M. Yang, X.P. Dong, Multipoint gas detection based on intrapulse absorption spectroscopy, IEEE Photon. Technol. Lett. 35 (20) (2023) 1086–1089.
[3] P. Mahbub, A. Noori, J.S. Parry, et al., Continuous and real-time indoor and outdoor methane sensing with portable optical sensor using rapidly pulsed IR LEDs, Talanta 218 (2020) 121144.
[4] A. Sampaolo, G. Menduni, P. Patimisco, et al., Quartz-enhanced photoacoustic spectroscopy for hydrocarbon trace gas detection and petroleum exploration, Fuel 277 (2020) 118118.
[5] Q. Wu, S. Nair, M. Shuck, E. Oort, et al., Advanced distributed fiber optic sensors for monitoring real-time cementing operations and long term zonal isolation, J. Petrol. Sci. Eng. 158 (2017) 479–493.
[6] Y.G. Wang, J.P. Sun, T. Li, et al., Multiplexed photonic crystal fiber gas-sensing network based on intracavity absorption, Sensors 22 (23) (2022) 9237.
[7] S.K. Danasegaran, E.C. Britto, S. Poonguzhali, Smart gas sensor based on photonic crystal for sensing perilous gases: industrial and mining applications, Energy Sources, Part A Recovery, Util. Environ. Eff. 44 (3) (2022) 7564–7572.
[8] X.L. Cai, X.J. Zhang, J. Fan, et al., Specific alcohol-responsive photonic crystal sensors based on host-guest recognition, Gels 9 (2) (2023) 83.
[9] R. Jannesari, T. Grille, G. Stocker, et al., Design of a narrow band filter based on a photonic crystal cavity for CO_2 sensing application, Sensors 23 (10) (2023) 4958.
[10] D.Q. Yang, X. Chen, X. Zhang, et al., High-Q, low-index-contrast photonic crystal nanofiber cavity for high sensitivity refractive index sensing, Appl. Opt. 57 (24) (2018) 6958–6965.
[11] C. Feng, G. Y, G.R. Feng, N.J. Zhou, S.H. Chen, Design of an ultracompact optical gas sensor based on a photonic crystal nanobeam cavity, Laser Phys. Lett. 9 (2012) 875–878.
[12] K. Schneider, P. Seidler, Strong optomechanical coupling in a slotted photonic crystal nanobeam cavity with an ultrahigh quality factor-to-mode volume ratio, Opt Express 24 (13) (2016) 263007.
[13] L. Kassa-Baghdouche, E. Cassan, High efficiency slotted photonic crystal waveguides for the determination of gases using mid-infrared spectroscopy, Instrum. Sci. Technol. (2017) 1–11.
[14] X. Shi, Z. Zhao, Z. Han, Highly sensitive and selective gas sensing using the defect mode of a compact terahertz photonic crystal cavity, Sensor. Actuator. 274 (2018) 188–193.
[15] M.G. Scullion, A.D. Falco, T.F. Krauss, Slotted photonic crystal cavities with integrated microfluidics for biosensing applications, Biosens. Bioelectron. 27 (1) (2011) 101–105.
[16] P. Saha, M. Sen, A slotted photonic crystal nanobeam cavity for simultaneous attainment of ultra-high Q-factor and sensitivity, IEEE Sensor. J. 18 (19) (2018) 3602–3609.
[17] S. Hu, S.M. Weiss, Design of photonic crystal cavities for extreme light concentration, ACS Photonics 3 (9) (2016) 1647–1653.
[18] F. Wang, C. Bertelsen, G. Skands, et al., Reactive ion etching of polymer materials for an energy harvesting device, Microelectron. Eng. 97 (2012) 227–230.
[19] K. Metwall, S. Queate, L. Robert, et al., Hot roll embossing in thermoplastic foils using dry-etched silicon stamp and multiple passes, Microelectron. Eng. 88 (8) (2011) 2679–2682.
[20] Z. Wang, Z.Y. Fu, F.J. Sun, et al., Simultaneous sensing of refractive index and temperature based on a three-cavity-coupling 380 photonic crystal sensor, Opt Express 27 (19) (2019) 26471–26482.
[21] J. Joannopoulos, S.G. Johnson, J.N. Winn, et al., Photonic Crystals:molding the Flow of light[M], Princeton University Press, 1995.
[22] P.T. Kristensen, C. Van Vlack, S. Hughes, et al., Generalized effective mode volume for leaky optical cavities, Opt Lett. 37 (10) (2012) 1649–1651.
[23] G.P. Kniffin, L.M. Zurk, Model-based material parameter estimation for terahertz reflection spectroscopy, IEEE Transactions on Terahertz Science and Technology 2 (2) (2012) 31–241.
[24] D. Bigourd, A. Cuisset, F. Hindle, et al., Detection and quantification of multiple molecular species in mainstream cigarette smoke by continuous-wave terahertz spectroscopy, Opt Lett. 31 (15) (2006) 2356–2358.

[25] World Health organization Report. www.(who.int&assets&pdf file&A).
[26] C.S. Goldenstein, V.A. Miller, R.M. Spearrin, et al., SpectraPlot.com: integrated spectroscopic modeling of atomic and molecular gases, J. Quant. Spectrosc. Radiat. Transfer 200 (2017) 249–257.
[27] R.V. Kochanov, I.E. Gordon, L.S. Rothman, et al., HITRAN Application Programming Interface (HAPI): a comprehensive approach to working with spectroscopic data, J. Quant. Spectrosc. Radiat. Transfer 177 (2016) 15–30.
[28] L. Li, H.Y. Hao, Simulated study of high-sensitivity gas sensor with a metal-PhC nanocavity via tamm plasmon polaritons, Photonics 8 (11) (2021) 506.
[29] A. Afsari, M.J. Sarraf, F. Khatib, Application of tungsten oxide thin film in the photonic crystal cavity for hydrogen sulfide gas sensing, Optik 227 (2021) 165664.
[30] N. Kumar, B. Suthar, C. Nayak, et al., Analysis of a gas sensor based on one-dimensional photonic crystal structure with a designed defect cavity, Phys. Scripta 98 (6) (2023) 065506.
[31] H.J. Zhao, High sensitivity refractive index gas sensing enhanced by surface plasmon resonance with nano-cavity antenna array, Chin. Phys. B 21 (8) (2012) 420–424.